Nanoparticle-Induced Packing Transition in Mesostructured Block Dendron−Silica Hybrids

Byoung-Ki Cho,*[,†,§] Anurag Jain,[†,§] Sol. M. Gruner,[‡] and Ulrich Wiesner*[,†]

Department of Materials Science and Engineering and Department of Physics and Cornell High Energy Synchrotron Source (CHESS), Bard Hall, Cornell University, Ithaca, New York 14853

Received October 27, 2006. Revised Manuscript Received April 17, 2007

Silica type nanostructured hybrid materials have been prepared by co-assembly of sol−gel materials and an extended amphiphilic dendron consisting of a hydrophilic aliphatic polyether block and hydrophobic docosyl chains. As confirmed by small- and wide-angle X-ray scattering (SAXS and WAXS) experiments, the hybrid preparation method employing simple solvent evaporation resulted in macroscopically oriented lamellar structures in which the docosyl groups crystallize normal to the lamellar plane. Contrary to a bilayer lamellar crystalline structure in the parent extended dendron, the hybrids show lamellar crystalline morphologies with an interdigitated monolayer packing of hydrophobic docosyl groups. This unusual structural transformation upon adding sol nanoparticles can be explained by alleviating an interfacial steric barrier for hydrophilic linear polyethers.

Introduction

The co-assembly of inorganic materials with organic amphiphiles has been envisaged as a platform for the next generation of functional materials with diverse potential applications ranging from drug delivery and single-particle tracking to photonics.[1] Linear macromolecular amphiphiles have been aggressively pursued as structure directing agents and templates to structure silica type inorganic materials at the nanoscale.[2−5] The combination of dissimilar and often incompatible components produces a host of novel structural features and property profiles in the resulting hybrid materials. Modification of the inorganic precursors[6−8] and molecular architecture of the organic components[9−11] have been the focus of more recent research for incorporating desired properties and structural features in the hybrids.

Amphiphilic dendrimers/dendrons present a distinct class of materials due to their unique structure and properties. The dense distribution of end functional groups for higher generations at the exterior of the dendrimer affords tremendous functionality, whereas the special molecular architecture is promising for obtaining novel well-defined structures at the nanoscale.[12] Since the pioneering work of Tomalia et al.,[13] dendrimers have been shown to possess fascinating phase behavior both in solution and bulk previously unknown in soft matter.[14−18] Similar to the dendrimer/dendron core, convergent[19] as well as divergent[20] (starburst) approaches have been developed for the synthesis of linear−dendritic diblock copolymers, which promise to further enrich the phase behavior of this class of materials. Despite their tremendous potential to structure direct, however, dendrimers have been used primarily as "porogens" in inorganic matrices, where they form spherical aggregates employed to generate well-defined pores in the surrounding continuous matrix.[21−24] In the present paper, we show that the specific

* Corresponding author. E-mail: chobk@dankook.ac.kr (B.-K.C.); ubw1@cornell.edu (U.W.).

† Department of Materials Science and Engineering, Cornell University.

§ Current address: Department of Chemistry and Institute of Nanosensor and Biotechnology, Dankook University, Seoul, Korea (B.K.C.); Intel Corporation, 5200 NE Elam Young Parkway, RA3-355 Hillsboro, OR 71245 (A.J.).

‡ Department of Physics and Cornell High energy Synchrotron Source (CHESS), Cornell University.

(1) Eckert, H.; Ward, M. D. *Chem. Mater.* **2001**, *13*, 3059.
(2) Zhao, D.; Feng, J.; Huo, Q.; Melosh, N.; Fredrickson, G. H.; Chmelka, B. F.; Stucky, G. D. *Science* **1998**, *279*, 548.
(3) Templin, M.; Franck, A.; Du Chesne, A.; Leist, H.; Zhang, Y.; Ulrich, R.; Schädler, V.; Wiesner, U. *Science* **1997**, *278*, 1795.
(4) Bagshaw, S. A.; Prouzet, E.; Pinnavaia, T. J. *Science* **1995**, *269*, 1242.
(5) Lu, Y.; Yang, Y.; Sellinger, A.; Lu, M.; Huang, J.; Fan, H.; Haddad, R.; Lopez, G.; Burns, A. R.; Sasaki, D. Y.; Shelnutt, J.; Brinker, C. J. *Nature* **2001**, *410*, 913.
(6) Garcia, C.; Zhang, Y.; DiSalvo, F.; Wiesner, U. *Angew. Chem., Int. Ed.* **2003**, *42*, 1526.
(7) Garcia, C. B. W.; Lovell, C.; Curry, C.; Faught, M.; Zhang, Y.; Wiesner, U. *J. Polym. Sci., Part B: Polym. Phys.* **2003**, *41*, 3346.
(8) Joo, S. H.; Choi, S. J.; Kwak, J.; Liu, Z.; Terasaki, O.; Ryoo, R. *Nature* **2001**, *412*, 169.
(9) Okabe, A.; Fukushima, T.; Ariga, K.; Aida, T. *Angew. Chem., Int. Ed.* **2002**, *41*, 3414.
(10) Cho, B.-K.; Jain, A.; Mahajan, S.; Ow, H.; Gruner, S. M.; Wiesner, U. *J. Am. Chem. Soc.* **2004**, *126*, 4070.
(11) Kimura, M.; Wada, K.; Ohta, K.; Hanabusa, K.; Shirai, H.; Kobayashi, N. *J. Am. Chem. Soc.* **2001**, *123*, 2438.
(12) Hawker, C. J.; Fréchet, J. M. J. *J. Am. Chem. Soc.* **1990**, *112*, 7638
(13) Tomalia, D. A.; Baker, H.; Dewald, J.; Hall, M.; Kallos, G.; Martin, S.; Roeck, J.; Ryder, J.; Smith, P. *Polym. J.* **1985**, *17*, 117.
(14) Grayson, S. M.; Fréchet, J. M. J. *Chem. Rev.* **2001**, *101*, 3819.
(15) Bosman, A. W.; Janssen, H. M.; Meijer, E. W. *Chem. Rev.* **1999**, *99*, 1665.
(16) Zeng, X.; Ungar, G.; Liu, Y.; Percec, V.; Dulcey, A. E.; Hobbs, J. K. *Nature* **2004**, *428*, 157.
(17) Cho, B.-K.; Jain, A.; Gruner, S. M.; Wiesner, U. *Science* **2004**, *305*, 1598.
(18) van Hest, J. C. M.; Delnoye, D. A. P.; Baars, M. W. P. L.; Van Genderen, M. H. P.; Meijer, E. W. *Science* **1995**, *268*, 1592.
(19) Gitsov, I.; Wooley, K. L.; Hawker, C. J.; Ivanova, P. T.; Fréchet, J. M. J. *Macromolecules* **1993**, *26*, 5621.
(20) Iyer, J.; Fleming, K.; Hammond, P. T. *Macromolecules* **1998**, *31*, 8757.
(21) Hedrick, J. L.; Hawker, C. J.; Miller, R. D.; Twieg, R.; Srinivasan, S. A.; Trollsås, M. *Macromolecules* **1997**, *30*, 7607.
(22) Kriesel, J. W.; Tilley, T. D. *Chem. Mater.* **1999**, *11*, 1190.
(23) Ruckenstein, E.; Yin, W. *J. Polym. Sci., Part A: Polym. Chem.* **2000**, *38*, 1443.
(24) Velarde-Ortiz, R.; Larsen, G. *Chem. Mater.* **2002**, *14*, 858.
(25) Jayaraman, M.; Fréchet, J. M. J. *J. Am. Chem. Soc.* **1998**, *120*, 12996.

10.1021/cm062564t CCC: $37.00
Published on Web 06/23/2007

Scheme 1. Molecular Structure and Phase Behavior of Extended Amphiphilic Dendron (transition temperatures given in °C; k_1, crystalline in ocosyl peripheries and PEO chains; k_2, crystalline only in docosyl peripheries; col_h, hexagonal columnar; dis, disordered)

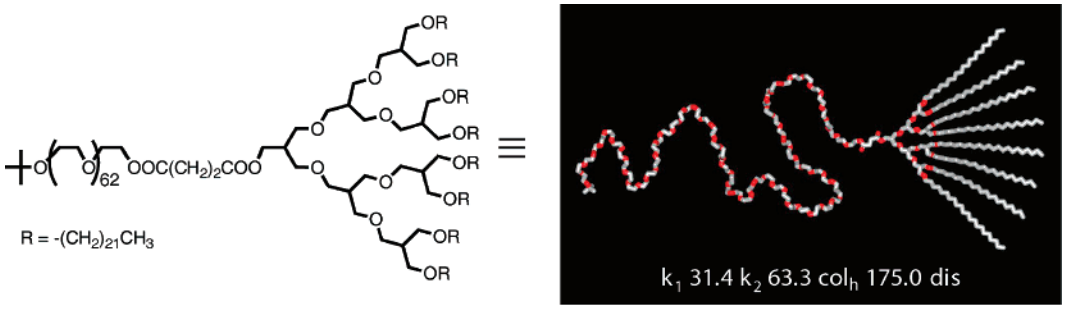

molecular architecture of an extended amphiphilic dendron results in unique structural features in nanostructured dendron−inorganic hybrids. In particular, we report on an inorganic nanoparticle-induced packing transition in dendron-based nanocomposites.

Experimental Sections

Reagents. Chloroform ($CHCl_3$), tetrahydrofuran (THF), aluminum *sec*-butoxide (from Fluka), (3-glycidylpropyl)trimethoxysilane (GLYMO, from Aldrich), and potassium chloride (KCl) were used as received.

Synthesis. The extended amphiphilic dendron used as a structure-directing agent was synthesized according to a procedure described in an earlier publication.[10] Organic−inorganic hybrids **a** and **b** were prepared from the extended dendron by similar procedures as described in reference 10.[27] For hybrid **a** (**b**), 107.0 mg (86 mg) of the extended dendron was dissolved in a mixture of 1 g of chloroform and 1 g of tetrahydrofuran. The solution was stirred for 1 h. Subsequently, a prehydrolyzed sol (150 mg (215 mg) for hybrid **a** (**b**)) of (3-glycidylpropyl) trimethoxysilane (GLYMO) and aluminum *sec*-butoxide (80/20 molar ratio) was added to the extended dendron-containing solution. The resulting mixture was stirred for 1 h and then poured into a petri dish covered with aluminum foil full of tiny holes. Evaporation of solvents was carried out at 63 °C. The resulting film was further heat-treated at 130 °C in a vacuum oven. Volatiles in the hybrid synthesis were evaporated at 63 °C in order for the sol−gel condensation to take place in the liquid crystalline phase and to suppress the docosyl chain crystallization, see text. Values of inorganic reported in the text were based on the amount of material remaining after evaporation of all the volatile components (estimated to be 55% of initial weight of the sol).[6] Volume fractions of the hydrophilic parts (hydrophilic dendritic core plus linear PEO chain plus aluminosilicate) in the hybrids were calculated using a density of 1.4 g/cm^3 for the PEO+inorganic phase.[27]

Methods. A Perkin-Elmer DSC-7 differential scanning calorimeter equipped with a 1020 thermal analysis controller was used to determine the thermal transitions and the heat of fusion. Small-angle X-ray scattering measurements were performed in transmission mode with a Rigaku rotating anode X-ray generator (Cu Kα, $\lambda = 1.54$ Å) focused by Franks mirror optics and operated at 40 kV and 50 mA. A 2D X-ray detector based on a 512 × 512 pixel Thomson CCD was used to acquire scattering patterns. The raw data was corrected for distortion and nonlinearity of the detector after background subtraction. It was then azimuthally integrated to obtain 1D plots of intensity vs scattering vector q

$$q = \frac{4\pi}{\lambda}\sin\left(\frac{\theta}{2}\right)$$

where θ = scattering angle and λ = wavelength of incident radiation. Wide-angle X-ray diffraction was performed on a Scintag $\theta-\theta$ diffractometer (Cu Kα, $\lambda = 1.54$ Å) operated at 45 kV and 40 mA. Atomic force microscopy samples were prepared by dip-coating a mica substrate in dilute solutions of nano-objects in toluene. The images were taken using a Veeco Nanoscope III Multimode scanning probe microscope employing tapping mode etched silicon tips.

Results and Discussion

The molecular structure of the parent extended amphiphilic dendron used as a structure-directing agent is shown in Scheme 1. A dendritic aliphatic polyether type core[25,26] is extended with a linear poly(ethylene oxide) (PEO) chain at the focal point. The synthesis of this compound was performed following a procedure reported earlier.[10] The overall molecular weight is 6000 g/mol with a polydispersity (M_w/M_n) of less than 1.05 as measured by gel permeation chromatography (GPC) and mass spectrometry.

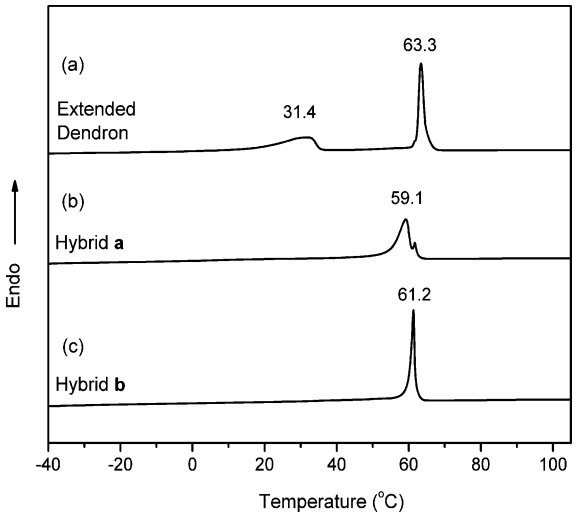

Figure 1. DSC thermographs of (a) the extended amphiphilic dendron, (b) hybrid **a**, and (c) hybrid **b**. In (a), the first transition at 31.4 °C corresponds to PEO melting, whereas the second transition at 63.3 °C corresponds to docosyl chain melting. In hybrids **a** and **b** ((b) and (c)), the crystalline melting transitions of docosyl peripheries occur at 59.1 and 61.2 °C, respectively, whereas no melting peaks for PEO are observed.

(26) Cho, B.-K.; Jain, A.; Nieberle, J.; Mahajan, S.; Wiesner, U.; Gruner, S. M.; Türk, S.; Räder, H. J. *Macromolecules* **2004**, *37*, 4227.
(27) Simon, P. F. W.; Ulrich, R.; Spiess, H. W.; Wiesner, U. *Chem. Mater.* **2001**, *13*, 3464.

Table 1. Thermal Characterization of the Extended Dendron and Hybrid Samples from DSC Data

	melting transtions (°C) with corresponding enthalpy changes in parentheses (J/g)	weight fraction of docosyl peripheries	normalized enthalpy change of docosyl peripheries (J/g)[a]
extended dendron	k_1 31.4 (39.1); k_2 63.3 (55.7)	0.41	135.9
hybrid **a**	k 59.1 (31.5)	0.23	137.0
hybrid **b**	k 61.3 (23.2)	0.17	136.5

[a] Normalized enthalpy of docosyl peripheries = enthalpy change/weight fraction of docosyl peripheries.

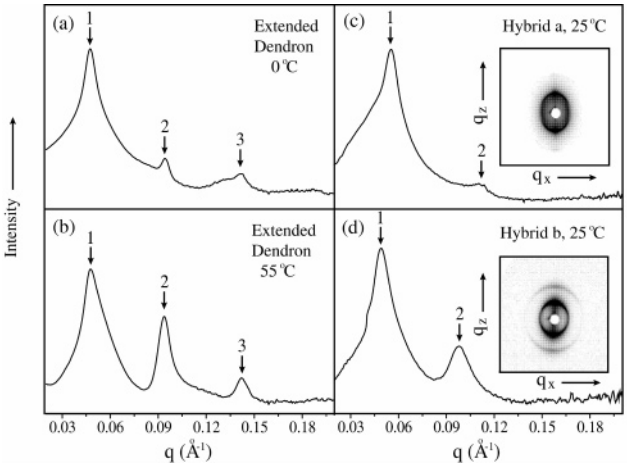

Figure 2. Small-angle X-ray scattering diffractograms for parent-extended dendron (a, b), hybrid **a** (c), and hybrid **b** (d) at temperatures as indicated in the figure. Insets in (c) and (d) show the 2D SAXS results. Tick marks in (a−d) are for lamellar lattices.

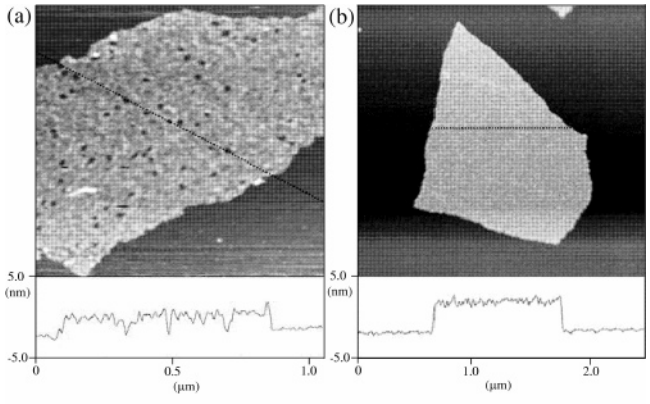

Figure 3. (a, b) AFM images from individual calcined nanoplates of hybrids **a** and **b** on mica, respectively. The two-dimensional profiles were recorded along the dashed lines in the images. For calcined nanoplates from **a** and **b**, the average layer thicknesses are 3.5 and 5.0 nm, respectively, which correspond to almost half the values estimated from SAXS. This reduction can be attributed to the significant volume shrinkage occurring during the calcination process in the AFM sample preparation procedure.[29]

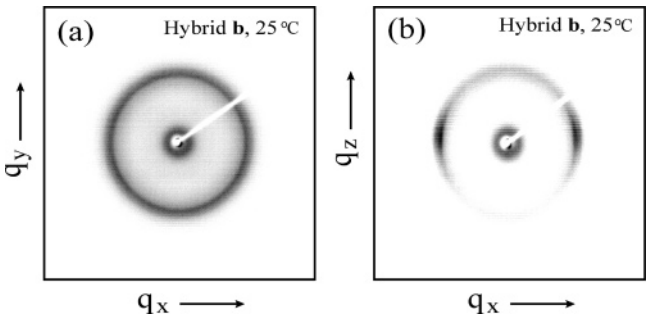

Figure 4. Wide-angle X-ray scattering diffractograms for two different film orientations of hybrid **b** (a, b). q_x, q_y, and q_z denote scattering wave vectors and the q_x-q_y plane is parallel to the sample film plane. The *d*-spacings of the reflections were estimated to be 4.13 Å.

On the basis of molecular density calculations, the volume fraction (*f*) of the hydrophilic part (dendritic core and PEO coil) of the parent extended dendron is 0.53. Its thermal behavior was studied by differential scanning calorimetry (DSC), small- and wide-angle X-ray scattering (SAXS and WAXS) and dynamic mechanical spectroscopy (DMS); results are summarized in Scheme 1. Two distinct DSC transitions at 31.4 and 63.3 °C were observed corresponding to melting of the linear PEO chains and docosyl peripheries, respectively (Figure 1a and Table 1). Upon further heating, this compound forms an ordered mesophase and finally disorders at 175 °C into a liquid. Each ordered crystalline phase was characterized by SAXS experiments. In the k_1 crystalline state, SAXS data show three reflections with *q*-spacing ratios of 1:2:3, consistent with a lamellar structure with a lattice parameter of 13.1 nm (Figure 2a). In the k_2 crystalline state after PEO melting, scattering data suggest that the lamellar structure persists (Figure 2b). Interestingly, the lamellar periodicity of 13.1 nm does not change going from k_1 to k_2. This is likely due to the fact that the molten PEO layers are confined between the crystalline docosyl layers. On the basis of the primary *d*-spacing and the length of a docosyl chain of 3.0 nm from a CPK model,[26] we expect the hydrophobic docosyl peripheries to self-assemble into a bilayer packing in both crystalline phases, see schematics in Figure 5a and b. Finally, above 63.3 °C, the SAXS pattern exhibits three reflections with *q*-spacing ratios of $1:\sqrt{3}:\sqrt{4}$, indicative of a hexagonal columnar mesophase with a lattice parameter of 12.1 nm (data not shown).

By loading different amounts of a prehydrolyzed sol of (3-glycidylpropyl) trimethoxysilane (GLYMO) and aluminum *sec*-butoxide to this extended dendron, we prepared two hybrid materials **a** and **b** as bulk films with volume fractions of the hydrophilic parts (hydrophilic dendritic core and PEO chain plus aluminosilicate) estimated as 0.70 and 0.77, respectively. From differential scanning calorimetry (DSC) measurements, as-made hybrid materials **a** and **b** show the crystalline melting transitions of docosyl peripheries at 59.1 and 61.3 °C, respectively, whereas no melting peaks for PEO are observed (Figure 1b and c). Furthermore, the normalized enthalpy changes of docosyl peripheries in the extended amphiphilic dendron and the hybrid samples as derived from the DSC measurements were nearly identical with values of about 136 J/g (Table 1). These observations suggest that microphase separation occurs between hydrophobic docosyl peripheries and hydrophilic regions, consisting of PEO chains mixed with the inorganic components resulting in a two-domain material similar to what is observed for linear macromolecular amphiphiles.[28]

SAXS experiments were performed on the as-made hybrid materials to corroborate this picture and to determine their

(28) De Paul, S. M.; Zwanziger, J. W.; Ulrich, R.; Wiesner, U.; Spiess, H. W. *J. Am. Chem. Soc.* **1999**, *121*, 5727.

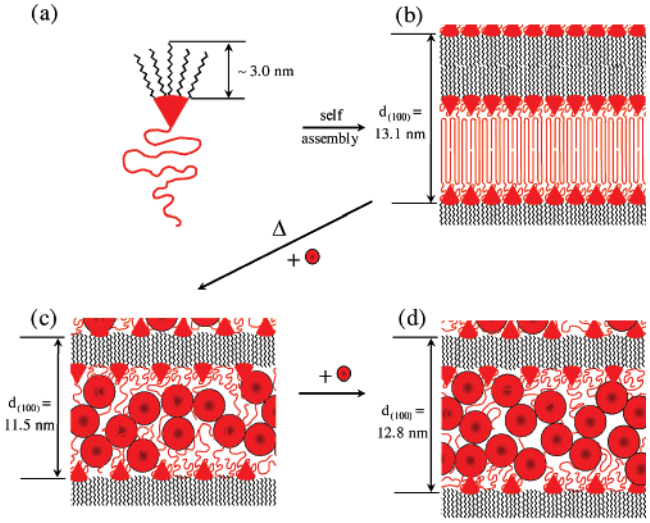

Figure 5. Schematic illustration of the packing transition induced by addition of the sol nanoparticles with typical diameters <5 nm.[29] Red and black regions represent hydrophilic and hydrophobic domains, respectively. Red spheres indicate prehydrolyzed sol nanoparticles. (a) Structural schematic of the parent extended dendron; (b) bilayer packing of docosyl peripheries in the crystalline states of the parent extended dendron; (c, d) molecular organization of sol particles and dimensions in hybrids **a** and **b**.

bulk morphology. Two-dimensional (2D) SAXS diffractograms of both hybrids show two-spot patterns with two reflections with a *q*-spacing ratio of 1:2 when the X-ray beam is incident parallel to the plane of the cast films (panels c and d of Figure 2). These results suggest lamellar morphologies for both hybrids. This interpretation was supported by atomic force microscopy (AFM) studies of the morphology of individual nanoparticles obtained from dissolution of the bulk materials. For imaging individually dispersed nanoparticles, solutions of hybrids **a** and **b** (5 mg of hybrid in 10 g of toluene) were ultrasonicated for 45 min, cast on freshly cleaved mica sheets, and calcined at 400 °C for 3 h. The representative AFM images in Figure 3 clearly identify lamellar sheets.

The 2D SAXS data in panels c and d of Figure 2 reveal that solvent-evaporation-induced co-assembly in these hybrids produces a preferred orientation of the lamellar normal parallel to the film normal, consistent with what is observed for block-copolymer-directed hybrids.[3] To characterize the orientation of the crystalline docosyl groups relative to the lamellar plane, WAXS experiments were performed for two different film orientations of hybrid **b** with respect to the X-ray beam at room temperature. An isotropic ring pattern was observed in the q_x-q_y plane (i.e., with the X-ray beam aligned normal to the film plane, Figure 4a), whereas two strong spots were evidenced in the q_x-q_z plane (Figure 4b). On the basis of the orthogonal relation between SAXS and WAXS data it can be concluded that the docosyl groups preferentially align along the lamellar normal.

On the basis of the primary *d*-spacings, i.e., $d_{(100)}$, obtained from the azimuthally integrated SAXS patterns in panels c and d of Figure 2, the lamellar periods for hybrids **a** and **b** were estimated to be 11.5 and 12.8 nm, respectively. Despite considerably increasing the hydrophilic volume fractions through addition of inorganic from 0.53 to 0.70/0.77, the lamellar *d*-spacings of the hybrids are surprisingly smaller than those in the crystalline states of the parent extended dendron. Although the thinning of the *d*-spacings can result from tilting of docosyl peripheries, the orientation evidence based on SAXS and WAXS data rules out this possibility. Thus, the reduction in lamellar thickness can be explained only by a fundamental change in the molecular organization of the hydrophobic peripheries (Figure 5). Assuming the length of a docosyl group to be ~3 nm,[26] the ratio of the hydrophilic layer thickness with respect to $d_{(100)}$ for the hybrids is consistent with their hydrophilic volume fractions. This strongly suggests that the peripheries in the lamellar structures of **a** and **b** self-assemble into an interdigitated monolayer packing, because molecular volumes are linearly proportional to primary *d*-spacings in lamellar structures.

The transformation from a bilayer to an interdigitated monolayer arrangement of the peripheries upon addition of inorganic sol nanparticles can be explained by relieving an interfacial steric barrier. In the crystalline states of the parent extended amphiphilic dendron, the molecular packing is dominated by the minimization of interfacial area because crystallization leaves the coil conformational freedom small, inducing the bilayer packing structure (Figure 5b). As shown in recent publications,[29,30] the sol−gel process proceeds through assembly of <5 nm silica type nanoparticles (sol) within the PEO domains. These sol particles may bring about a significant steric hindrance between PEO chains in a bilayer packing model. On the contrary, the transformation into an interdigitated monolayer arrangement provides a way to reduce the interfacial steric barrier, because the cross-sectional area occupied by a PEO chain is larger than that in a bilayer packing (compare diagram b with diagrams c and d in Figure 5).

Conclusions

Nanostructured hybrid materials have been prepared through co-assembly of an extended amphiphilic dendron and silica-type sol nanoparticles. The hybrid preparation procedure employing solvent evaporation yielded macroscopically oriented lamellar films. In contrast to a bilayer lamellar structure in the parent extended amphiphilic dendron, structural data on these hybrids suggest lamellar morphologies with an interdigitated monolayer packing of hydrophobic peripheries. This packing transition can be rationalized by reducing interfacial steric barrier induced by the addition of sol nanoparticles.

Acknowledgment. This work was supported by the Postdoctoral Fellowship Program of the Korea Science & Engineering Foundation (KOSEF) and the National Science Foundation (DMR-0312913). Financial support of Philip Morris, USA, is gratefully acknowledged. The SAXS X-ray facility is supported by the Department of Energy BER Grant DE-FG02-97ER62443. This work made use of the Cornell Center for Materials Research Hudson mesoscale facility, supported through the National Science Foundation Materials Research Science and Engineering Centers Program (DMR-0079992). We thank H. J. Räder and S. Türk at the Max-Planck Institute for Polymer Research for the MALDI-TOF measurements on the extended dendron.

CM062564T

(29) Jain, A.; Wiesner, U. *Macromolecules* **2004**, *37*, 5665.
(30) Warren, S. C.; DiSalvo, F. J.; Wiesner, U. *Nat. Mater.* **2007**, *6*, 156.